

This is the submitted version of the article “Impact of Chemical Composition on 3D Elemental Distribution and Damage Behavior of Cast Al-Si Alloys”, published in *Microsc. Microanal.* 28 (Suppl 1), 2022, © Microscopy Society of America 2022, doi:10.1017/S1431927622001878. Published online by Cambridge University Press.

Impact of Chemical Composition on 3D Elemental Distribution and Damage Behavior of Cast Al-Si Alloys

Katrin Bugelnig^{1*}, Holger Germann², Thomas Steffens², Fabian Wilde³ and Guillermo Requena^{1,4}

¹. Institute for Materials Research, German Aerospace Center (DLR), Cologne, Germany

². KS Kolbenschmidt GmbH - Neckarsulm, Germany

³. Helmholtz-Zentrum Hereon - Geesthacht, Germany.

⁴. RWTH Aachen University – Aachen, Germany.

* Corresponding author: katrin.bugelnig@dlr.de

Cast Al-Si alloys are the most suitable choice for automotive piston applications due to their high strength-to-weight ratio, excellent castability and heat conductivity. However, the rising demand for more efficient combustion engines, pushed by environmental regulations, is leading to thermo-mechanical conditions at the limits of operability of conventional Al-Si piston alloys [1]. As such, piston alloys are subject to continuous developments towards improved performance without losing the lightweight advantage and recyclability provided by Al alloys. The microstructure of cast Al-Si piston alloys consists of an α -Al matrix and interconnected 3D hybrid networks formed by eutectic/primary Si as well as Ni-, Cu-, Mg- and Fe-rich intermetallic phases. These networks play a decisive role on damage retardation of cast Al-Si alloys, as shown recently by the authors [2,3]. Particularly, the intermetallic phases γ -Al₇Cu₄Ni, δ -Al₃NiCu and β -Al₅FeSi determine the strength and damage behavior at room and elevated temperatures [4,5,6].

This study aimed at determining the 3D elemental distribution of Cu and Ni as a function of alloy composition to evaluate their effect on fraction and stability of γ , δ and β intermetallics. Moreover, a direct correlation between the 3D spatial distribution and data from in-situ tensile tests allows identifying microstructural constituents that induce/retard damage initiation/accumulation during deformation. To this purpose, synchrotron tomography experiments were carried out at the P05 Microtomography beamline at PETRA III, DESY in Hamburg, Germany. First, absorption edge tomography was applied to determine the 3D distribution of Cu and Ni within intermetallic phases and then, microtomography was carried out in situ during tensile testing. Experimental observations have also been complemented by thermodynamic simulations using the Thermo-Calc software.

Thermodynamic simulations reveal that the fraction and stability of phases is related to the Fe/Ni content and Fe:Ni ratio. Thus, 2 alloys which were expected to result in varying volume fractions of the γ , δ and β phases according to our calculations considering thermodynamic equilibrium were studied. In real alloys phase fractions and homogeneity may vary from these theoretical estimations. It is therefore imperative to identify the 3D distribution of aluminide-forming elements to fully understand the mechanical behavior and further improve the design of aluminide-reinforced alloys. Absorption-edge X-ray tomography allows 3D elemental sensitive imaging by scanning the alloys above and below the X-

ray absorption edges of Ni and Cu, allowing the combined 3D investigation of elemental distribution and phase morphology. Since Cu and Ni are present in the γ and δ phase, they can be identified by this technique and the homogeneity of their 3D distribution, i.e. the phase thermal stability, can be determined. Since the β -phase does not contain Ni or Cu, it can also be identified. Moreover, damage in Al-Si alloys initiates and evolves in a rather localized manner, which makes 3D imaging necessary to univocally follow the damage process and correlate it with the actual microstructure 3D architecture.

The tomography experiment was conducted as follows:

1. Tomography scans below and above the X-ray absorption edges of Ni and Cu (8.3328keV and 8.9789keV, respectively) were taken for two cast Al-Si alloys with different Ni, Cu, Fe contents.
2. Afterwards, the beam energy was increased to 20keV to obtain best quality tomographic scans at reasonable scan times for the in-situ tensile tests. Figure 1 shows the experimental setup.

Figure 2 shows representative reconstructed 2D slices of the same sample at the same position for different energies for an AlSi12Cu4Ni2Mg alloy. A 2D reconstructed slice of the sample in post-mortem condition gives first impression of the role of varying phases regarding propagation of the main crack during tensile deformation. For further 3D investigations, image segmentation of the acquired in situ datasets was supported by a deep learning approach using convolutional neural networks [7].

This study enabled us to identify intermetallic phases in tomographic images and also revealed the correlation between the 3D elemental distribution within intermetallics and the damage evolution in the investigated alloys.

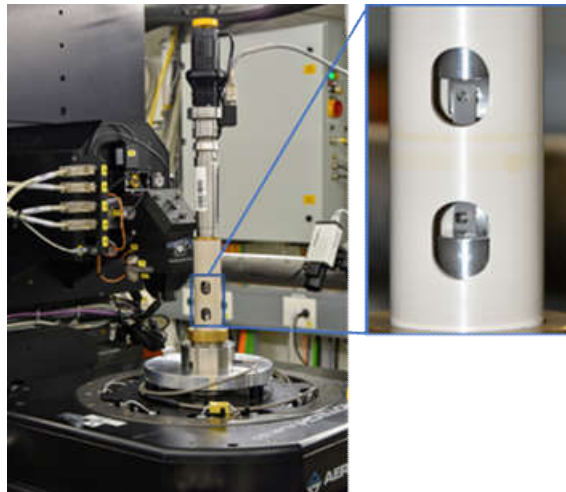


Figure 1. experimental setup for tomography experiments.

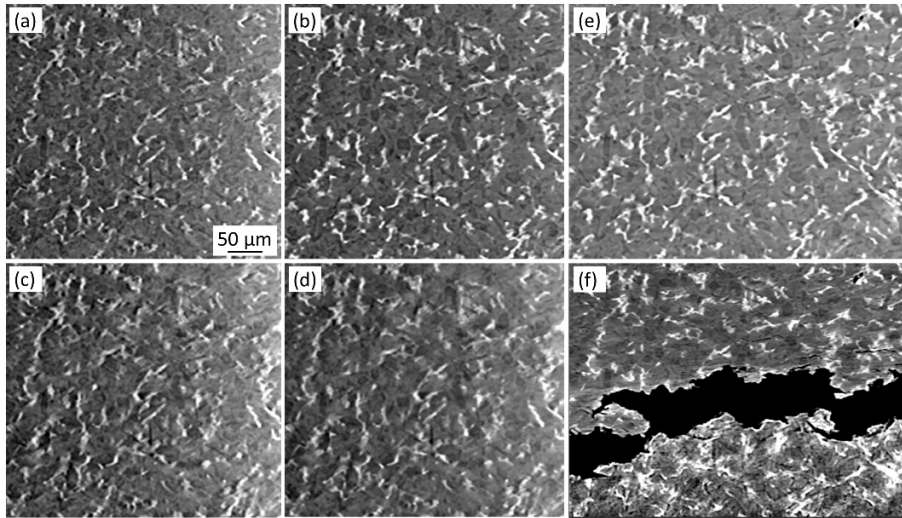


Figure 2. reconstructed 2D-slices acquired at energies of (a) 8.310keV (below Ni-edge), (b) 8.350keV (above Ni-edge), (c) 8.960keV (below Cu-edge), (d) 9.0keV (above Cu-edge) and (e) 20KeV for an AlSi12Cu4Ni2Mg alloy. (f) post-mortem condition (same sample/same position).

References:

- [1] The European Parliament and the Council of the European Union, Directive 2000/53/EC of the European Parliament and the Council of 18 September 2000 on End-of-Life Vehicles, (2000), p. 34-42.
- [2] K. Bugelnig et al., *Mat. Sci. Eng. A* 709 (2018), p. 193-202.
- [3] K. Bugelnig et al., *Materials* 11(8) (2018), p. 1300.
- [4] Z. Asghar et al., *Acta Materialia* 59 (2011), p. 6420-6432, doi: 10.1016/j.actamat.2011.07.006.
- [5] X. Cao et al., *Materials Transactions* 47(5) (2006), p. 1303-1312.
- [6] Y. Liu et al., *Anal. Bioanal. Chem.* 404 (2012), p. 1297–1301, doi: 10.1007/s00216-012-5818-9.
- [7] T. Strohmam et al., *Scientific Reports* 9 (2019), 19611, doi: 10.1038/s41598-019-56008-7.
- [8] The authors acknowledge the DESY for the provision of synchrotron radiation facilities in the framework of the proposal I-20190900.